AN ABSTRACT OF THE THESIS OF

Charles Fredric Greenlaw III for the degree of Master of Science

in Physical Oceanography presented on May 10, 1976

Title: Acoustic Backscattering from Marine Zooplankton

Abstract approved: Redacted for Privacy

Richard K. Johnson

Target strengths for preserved specimens of three common zooplankters--a copepod (C. marshallae), an euphausiid (E. pacifica), and a sergestid shrimp (S. similis)--were measured in a fresh-water tank in the laboratory. Data were taken at eight frequencies from 220 kHz to 1100 kHz and for limited size ranges of the plankters.

Measurements were compared to target strengths predicted from a fluid sphere scattering model, which has been used in the past to predict scattering from planktonic organisms. Certain predictive ability was found for this model, but only for limited frequency and size ranges and--in the case of the euphausiids and sergestid shrimp--only for certain aspect angles. Above a critical value of ka (about 1.5 for the copepods and about 10 for the euphausiids) the observed target strengths increased significantly above the predicted levels, suggesting that spherical harmonic modes were no longer adequate to describe the scattering process. In addition, the sergestid shrimp and euphausiids were found to be directional, with maximum target

strengths at side or dorsal aspects and minimum target strengths at anterior aspect. The fluid sphere model does not predict directional backscattering.

The partial agreement of measured and predicted target strengths suggests that the assumption of a fluid scatterer is valid, but directional backscattering implies that a spheroid would be a better shape. A spheroid model might also predict the increase in target strength at higher ka that was observed in these measurements. All of the specimens measured in this study are physically representable as prolate spheroids of different eccentricities. It is proposed that a fluid prolate spheroid might be a better model to predict scattering from marine zooplankton.

Acoustic Backscattering from Marine Zooplankton

by

Charles Fredric Greenlaw III

A THESIS

submitted to

Oregon State University

in partial fulfillment of
the requirements for the
degree of

Master of Science

Commencement June 1976

APPROVED:

Redacted for Privacy

Assistant Professor of Oceanography

Redacted for Privacy

Dean of the School of Oceanography

Redacted for Privacy

Dean of Graduate School

Date thesis is presented May 10, 1976

Typed by Martha Greenlaw for Charles Fredric Greenlaw III

ACKNOWLEDGMENTS

Several persons contributed valuable assistance during this research. Most of the specimens used in the measurements were provided by Joanne Laroche and Earl Krygier. Some of the displacement volume and length measurements of euphausiids were made by Harriet Lorz. Barbara Dexter measured the thicknesses of several euphausiid molts at my request. Professor Leland Jensen allowed the use of his tank facilities for calibration of the transducers.

Special acknowledgment must be made to Richard Johnson, who provided direction, guidance, encouragement, and enthusiasm when it was most needed; to Charles Miller, who managed to make biology interesting to me; to my wife, who provided constant encouragement and support during the research and the preparation of this thesis; and to my son, who has waited eighteen months for his father to take him fishing.

TABLE OF CONTENTS

LIST OF ILLUSTRATIONS

ACOUSTIC BACKSCATTERING FROM MARINE ZOOPLANKTON

I. INTRODUCTION

Remote acoustical sampling of biomass in the sea or in lakes has been an elusive goal for many years. The discovery that the deep scattering layers observed worldwide in the oceans were caused by scattering from biological organisms (1) suggested acoustical sampling as a means of making rapid, large area surveys of biomass, either as an adjunct to or a substitute for conventional net sampling.

Association of zooplankter concentrations with scattering layers has been reported for low frequency (<30 kHz) measurements (2) as well as for higher frequency measurements (3 - 10). Measurements made at sea could not be confined to homogeneous populations of particular plankters, of course, so these associations were generally qualitative and not a little speculative. Northcote (3) measured scattering layers in a shallow lake with a fish population that was artificially maintained and subject to periodic winterkill. The remainder of the life-forms in the lake consisted of few species of copepods, cladocerans, and chaoborids. Clear associations between the chaoborid larvae vertical distributions and the (200 kHz) echo sounder traces were found, suggesting that these larvae were the principal cause of scattering at this frequency. It should be noted that chaoborid larvae are unusual plankters in that they possess small air sacs, which enhance the acoustical scattering.

Barraclough, LeBrasseur, and Kennedy (5) operated a high frequency (200 kHz) echosounder during two crossings of the North Pacific, making periodic net tows to sample the observed scattering layers. At

night the net hauls consisted of a mix of nekton and plankton. The daytime hauls in the shallow scattering layers consisted of some 99 percent copepods (Calanus cristatus). Remarkable agreement between scattering layer depths and the depths of maximum copepod concentration was found. Quantitative data on biomass was presented, but the acoustic system was apparently unsuitable for making comparisons with the biological data records.

Quantitative estimates of biomass have been made by McNaught (7), who measured acoustic scattering at five frequencies in the Great Lakes. He obtained regression relations between biomass estimates from concurrent net tows and integrated voltage outputs from his acoustic sampler.[1] His data, of necessity, cover heterogeneous populations of plankters; that is, plankters of different species, sizes, and so forth.

Beamish (8) measured scattering in Saanich Inlet, British Columbia, in waters dominated by the euphausiid, Euphausia pacifica. From net haul estimates of abundance, he calculated a scattering cross section for E. pacifica at the frequency of his measurements. Somewhat later, Pieper (9) measured acoustical backscattering at three frequencies in the same region. He found clear association between backscattering and biomass and between backscattering strength and frequency.

McNaught and Beamish invoked a scattering model in their reports, the former to justify his technique and choose the frequencies of

---

[1]The reported regression relations are in error; McNaught, personal communication.

operation and the latter to explain the causes of the scattering of the zooplankters. The model used was that for scattering from a fluid sphere.

More recently, Castile (10) measured near-surface backscattering at 330 kHz in the Western Pacific. The fluid sphere model was used to speculate about probable causes of the observed scattering, as no associated biological sampling was undertaken.

It is commonly assumed that the fluid sphere scattering model is probably an accurate predictor for the acoustical scattering from zooplankton under certain conditions (principally, frequencies such that the wavelength is larger than the maximum dimensions of the scatterer). This assumption has never, to the author's knowledge,[2] been tested by measuring backscattering for marine zooplankton over a range of frequencies and/or sizes and comparing the results with the fluid sphere predictions.

The present work was undertaken to determine the scattering characteristics of representative marine zooplanktons over a range of frequencies, with one objective being a test of the fluid sphere model. Individual specimens of three dominant zooplankters were measured; the copepod, Calanus marshallae, the euphausiid, Euphausia pacifica, and the sergestid shrimp, Sergestes similis.

---

[2]Some measurements of squid, sea bass, and two species of large shrimp were made by Smith (11) in 1954, over the frequency range 8 to 30 kHz. His data for the shrimp were inconclusive.

For experimental convenience, preserved specimens were used and the acoustical measurements were made in fresh rather than in sea water. The absolute target strengths are not, therefore, directly applicable to in situ measurements. The physical properties thought to be relevant to acoustic scattering (density and sound speed) were determined for samples of the zooplankters used in the acoustical measurements, however, so that appropriate values could be used in the fluid sphere calculations. It is believed that the effects of preservation and measurement in fresh water were of no importance in assessing the gross behavior of the acoustical backscattering, which was the principal goal of this work.

II. SCATTERING MODELS

A model for scattering behavior is useful for many reasons. From a model which accurately predicts scattering from one species of plankter, the scattering from other species similar in the acoustical properties may be predicted with some confidence. With a proper model, scattering from different sizes of the same plankter can be predicted. If directional scattering characteristics are modeled, then average scattering strengths for populations of random aspects can be predicted. If the scattering model predicts scattering spectra with some "character," such as sharp peaks at certain frequencies, then wideband measurements of (simple) populations might be of use as clues to identification of the scatterers. Hence, the possibility exists that a certain amount of acoustic sampling of biological assemblages might be made and estimates formed of the size distributions and biomass--remotely and over large regions of space and time and without the need for extensive net sampling.

Models to describe the acoustical backscattering behavior of zooplankton can be operationally classed into two groups--those that treat the plankter as a constrained volume of fluid with properties just slightly different from the surrounding medium, and those which treat the scatterer as an elastic body. In either group, spherical shapes are preferred, as the mathematics are simpler, but spheroids are reasonably tractable on digital computers. The reason for grouping models as fluid or elastic rather than by shape is that the additional elastic constants--shear moduli, Poisson's ratio, shear wave

velocity--required for elastic models are almost wholly unknown for zooplankton (12). In addition, measurement of the elastic constants would be quite difficult for planktonic organisms.

Traditionally, the fluid sphere model has been invoked by researchers to explain their data (7 - 10). Further, low frequency approximate relations were usually employed as these are much simpler than exact solutions and can be used without the aid of a computer. Typical plankters are seldom even approximately spherical, the dominant plankton are usually crustaceans with chitinous exoskeletons, and it simply is not known whether the body tissues (which can contain inclusions of oils, stomach contents of skelatinous material, etc.) are fluid-like or elastic materials. The difficulties associated with the other models and the reasonable behavior of the fluid sphere model, though, have so far made this seem a reasonable choice.

The fluid sphere model is described in the following section; other models that seem pertinent are discussed briefly in the succeeding section.

A. The Fluid Sphere

A fluid medium is defined as one which does not support shear waves. For acoustic problems, this means that the only relevant physical properties are density and bulk compressibility--or, what is the equivalent, density and bulk compressional wave speed. For discrete scatterers, the remaining physical quantity(s) necessary for acoustic description is dimension(s). Anderson's (13) solution for scattering from a fluid sphere is a function of these properties of the sphere

and similar properties of the medium. In his solution, as in the other, approximate forms (14, 15) and in Machlup's (16) model with a shell, the equations are written such that the densities and sound speeds occur as contrasts--the ratios of these properties in the scatterer to their values in the surrounding medium.

Anderson's solution is for the reflectivity of a fluid sphere, where reflectivity is defined as the ratio of the scattered pressure magnitude to that which would be scattered from a perfectly reflecting sphere of the same size (in all directions, uniformly). In symbolic form,

$$R = R(ka, g, h)$$

where

ka = the wavenumber ($2\pi/\lambda$) in the medium times the radius of the sphere

g = the ratio of densities (sphere to medium)

h = the ratio of sound speeds (sphere to medium).

The reflectivity equation is a complicated infinite series of spherical Bessel functions of the first and second kind and Legendre polynomials. It will not be reproduced here. Although R is a complex function, phase will not be considered and only magnitudes will be treated.

The quantity measured in these experiments and in most measurements of single targets is target strength (TS). TS is defined as the ratio of the scattered intensity from a scatterer, referred to 1 meter from the acoustic center of the target, to the intensity of the wave incident on the scatterer. Customarily, TS is expressed in decibel form

$$TS = 10 \log(I_s/I_i) \quad \text{(at 1 meter)}.$$

Intensity is proportional to the square of pressure amplitude, so an equivalent expression would be

$$TS = 20 \log (P_s/P_i) \quad \text{(at 1 meter)}.$$

With some manipulation, a relation for TS in terms of the reflectivity can be obtained

$$TS = 10 \log(R^2a^2/4),$$

where a is the geometric radius of the spherical scatterer in meters. For the purposes of these measurements, it was convenient to compute the reflectivities in nondimensional form so that a single prediction curve could be used for scatterers with similar properties but of different sizes. A reduced target strength was defined for the theoretical predictions as the target strength of a fluid sphere of the given g and h values, but 1 mm in radius. That is, the quantity

$$TS' = 20 \log(R) - 66 \text{ dB} \qquad (1)$$

was calculated from Anderson's expression for R with the predicted values of g and h and plotted versus ka. Measured target strengths were scaled to the TS' axis by

$$TS' = TS - 20 \log(a)$$

and $k\hat{a}$ used to estimate ka, where $\hat{a}$ is the radius of an equivalent volume sphere. (See Section III.)

A plot of TS' versus ka is given in figure 1. The parameters g and h are those estimated for the acoustic measurements of the euphausiid and sergestid shrimp in fresh water. Two features are worth noting. First, at values of ka much less than 1, the curve is nearly linear with a slope proportional to $(ka)^4$. Many approximate solutions for low ka exhibit this feature, such as the approximation of Rayleigh (14), and this is the scattering law for rigid spheres. Second, at high values of ka, there is a more or less constant mean value of TS' about which the curve varies. The spacing between peaks (or nulls) of this pattern of ripples is reasonably constant at just over 2 ka/peak.

Anderson obtained an approximate form for the reflectivity function in the limit of ka approaching 0,

$$R^2 \simeq 4(ka)^4 \left[\frac{1 - gh^2}{3gh^2} + \frac{1 - g}{1 + 2g}\right]^2 . \qquad (2)$$

The approximation due to Rayleigh is equivalent but uses compressibility ratios ($\kappa = 1/\rho c^2$) instead of sound speed ratios. The dashed curve in figure 1 is reduced target strength calculated from equation 1 using the approximate relation, equation 2. It can be seen that the difference between the exact and approximate relations is small at low ka and is still only a factor of 2 larger (+6 dB) at ka of approximately 0.8.

A modification of the fluid sphere model was made by Machlup (16), who considered the scattering from a fluid sphere with a thin elastic

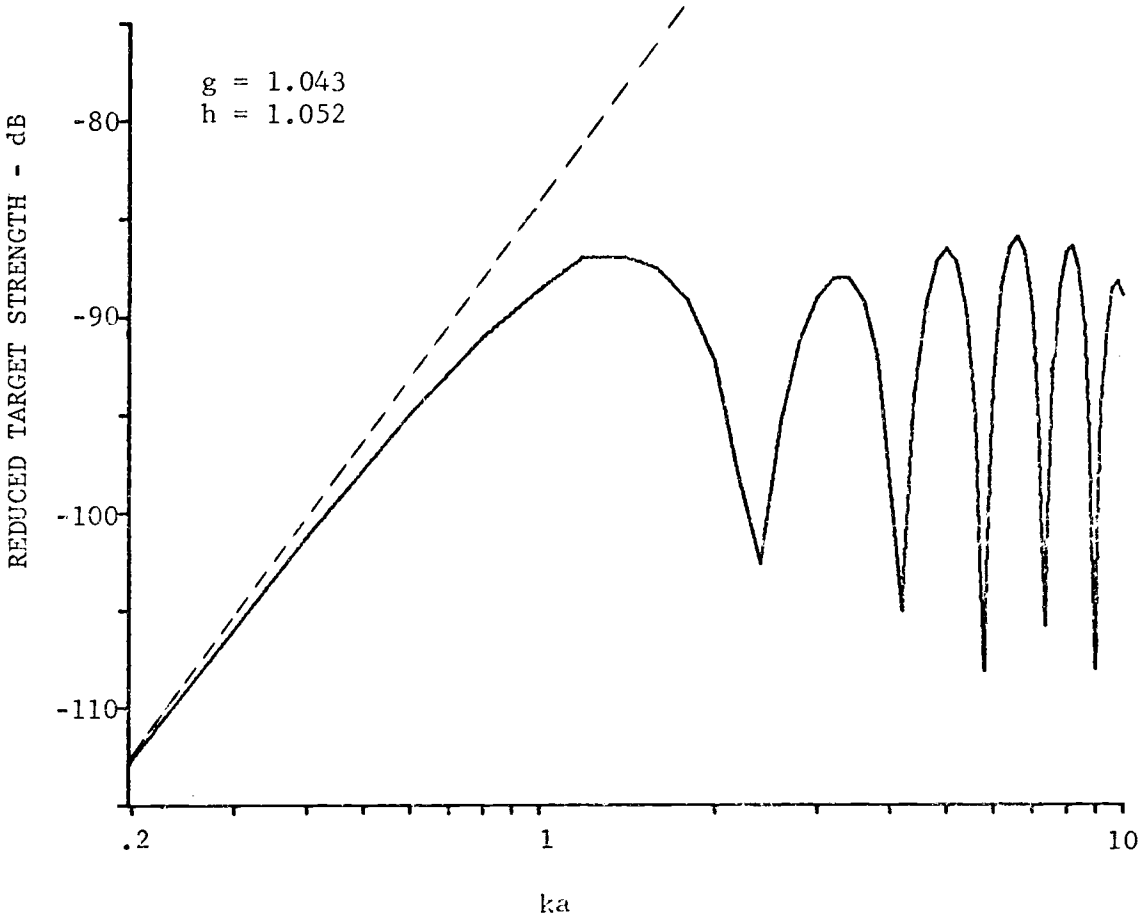

Figure 1. Reduced target strength versus ka, fluid sphere model.

shell. He concluded that thin shells were of no effect in the region of ka equal 1 and might reduce the scattering strengths somewhat at ka less than 1. He did not present the solution for higher frequencies, nor did he justify the particular choice of elastic constants used in an example. Machlup noted, however, that

> the irregular shape of (marine crustaceans) would tend to eliminate the strong flexural modes of vibration of which the sphere is capable. On the other hand, the segmented character of their carapace may permit the low frequency flexural modes possible for a short cylinder.

It must be remarked that his calculations used a ratio of shell thickness to sphere radius of 1/500, which implies a carapace some five times thicker than the carapace of euphausiids.[3]

No spherical model will predict aspect-dependent scattering behavior.

B. Other Models

Many zooplankters are elongate, resembling prolate spheroids to some degree. A reasonable next approximation from the fluid sphere might be a fluid prolate spheroid. A solution to the scattering from such a body was obtained by Yeh (17). Numerical examples of the effect of the aspect angle of the spheroid on the backscattering were presented for a few cases, showing generally that backscattering was greatest for broadside incidence. At other aspects, the scattering strength was lower and varied with angle from broadside. Predicted

---

[3]B. Dexter, OSU, personal communication.

backscattering strength for end-on incidence in the two cases considered was some 10 percent to 20 percent of that at broadside. No data on the backscattering spectra were presented.

Intuitively, the fluid prolate spheroid model has much appeal. A spheroid is a much better physical representation of a zooplankter, and the shape surely is important at least at high frequencies. Observation of directional scattering from the zooplankton would be further evidence that a nonspherical shape was a better model.

Elastic scatterers have been studied by many investigators; the elastic sphere by Hickling (18) and Lebedeva (19) most recently, the elastic cylinder (20, 21), and other shapes for which the wave equation is separable. In the absence of information about the elastic constants of zooplankton, no predictions from these models are possible. Lebedeva's solution was expressly tailored for scattering from zooplankton at low ka, considering the scatterers as both monolithic elastic spheres and as elastic spheres with shells of different elastic properties. Using her own data (12) on elastic constants of fish tissues, and approximating the shear modulus of chitin by that for horny tissue, she calculated low (but unspecified) frequency scattering cross sections for euphausiids and sergestid shrimp. Polar diagrams of the scattering at different shell thicknesses showed an increase in backscattering strength with increasing shell thickness. This is more or less in accord with Machlup's model, for which he claimed a small reduction in scattering strength for a thin shell at low ka.

III. PHYSICAL MEASUREMENTS

Three parameters characteristic of the plankter are needed to predict its acoustic scattering with the fluid sphere model; the density, bulk sound speed, and the radius of the "sphere." The fluid sphere model was exercised for various values of g and h near those observed in the acoustic measurements, with these results: for h of 1.07, changing g from 1.00 to 1.03 (uniformly) increased TS' by less than 2 dB; for g of 1.03, changing h from 1.07 to 1.10 increased TS' (less uniformly, since the location of the peaks and valleys moved slightly) by 4 dB. Considering the measurement errors and specimen-to-specimen variations expected, it was concluded that differences between measurements and predictions of these magnitudes could not be regarded as significant. The methods used to measure these physical parameters (described in the appendix) are considered more than sufficiently accurate for the purposes at hand.

A. Specimens

Preserved specimens of zooplankters commonly found in the Eastern Pacific off Oregon were obtained for measurement. The dominant zooplankters, at various places and various times of the year, are copepods, euphausiids, and sergestid shrimp. Samples of these zooplankters, collected in mid-summer of 1975 and preserved in 5 percent buffered formalin, were selected from the collections for the acoustic measurements and for the physical measurements (Appendix). The euphausiids were sized (total lengths, posterior edge of the occipital notch to

tip of telson, were used, and only undamaged specimens selected) and placed in individual specimen bottles for identification in the acoustic measurements. The sergestid shrimp were similarly treated. Subsamples of the copepods were examined for size estimates but kept en masse in a single container. Only single species were used: Euphausia pacifica (euphausiids), Sergestes similis (sergestid shrimp), and Calanus marshallae (copepod).

B. Density

The densities of preserved specimens of the euphausiid and copepod were measured at two temperatures, 9.4°C and 19°C. Densities for other euphausiids (same species, but not included in the acoustic measurements) were made on both fresh specimens and the same specimens after preservation. Density for the sergestid was measured at only one temperature.

Mean density for the preserved copepods was 1.046 gm/ml at 9.4°C and 1.045 gm/ml at 19°C. The ranges (95 percent confidence intervals) were nearly identical; 1.037 to 1.057 gm/ml at the low temperature and 1.035 to 1.055 gm/ml at the high temperature. It was noted that the copepods contained variable amounts of oil in their oil sacs and that specimens with more oil tended to be less dense. Since the interval between density bottles was 0.005 gm/ml, the difference between mean values of density is solely due to distributional differences. Probably the density varies with temperature, but the change appears to be less than the precision of these estimates.

The densities of fresh specimens of euphausiids were measured in

August, 1975. The mean density of 54 samples was 1.063 gm/ml at 7.4°C. After preservation for several months, the densities of a subsample of the same euphausiids were measured. At both 9.4°C and 19°C, the mean density was 1.043 gm/ml. Again, the effect of temperature appears to be less than the precision of the estimate. It is interesting to note that preservation decreased the density of the specimens by about 2 percent.

Densities of the sergestid were measured at 15.8°C only. The mean value was 1.051 gm/ml. During the measurements, it was observed that the sergestids consistently floated head up, suggesting that the thoracic region was less dense than the abdomen. A number of specimens were cut in half at the juncture of the thorax and abdomen, and the densities remeasured. It was found that the mean densities for abdominal parts alone was 1.059 gm/ml and 1.040 gm/ml for the thoracic parts. The standard errors were less than a density interval in each case, so the differences are significant. The lesser density of the thorax possibly reflects the presence of oil, although it may simply be due to the presence of all of the vital organs in the thorax and a preponderance of muscle in the abdomen.

C. Sound Speeds

Sound speeds were measured in a velocimeter at several temperatures near 10°C for the copepods and euphausiids and near 20°C for all specimens.

Five measurements of sound speed were made for copepods, at temperatures from 9.5°C to 18.5°C. The results are shown in figure 2.

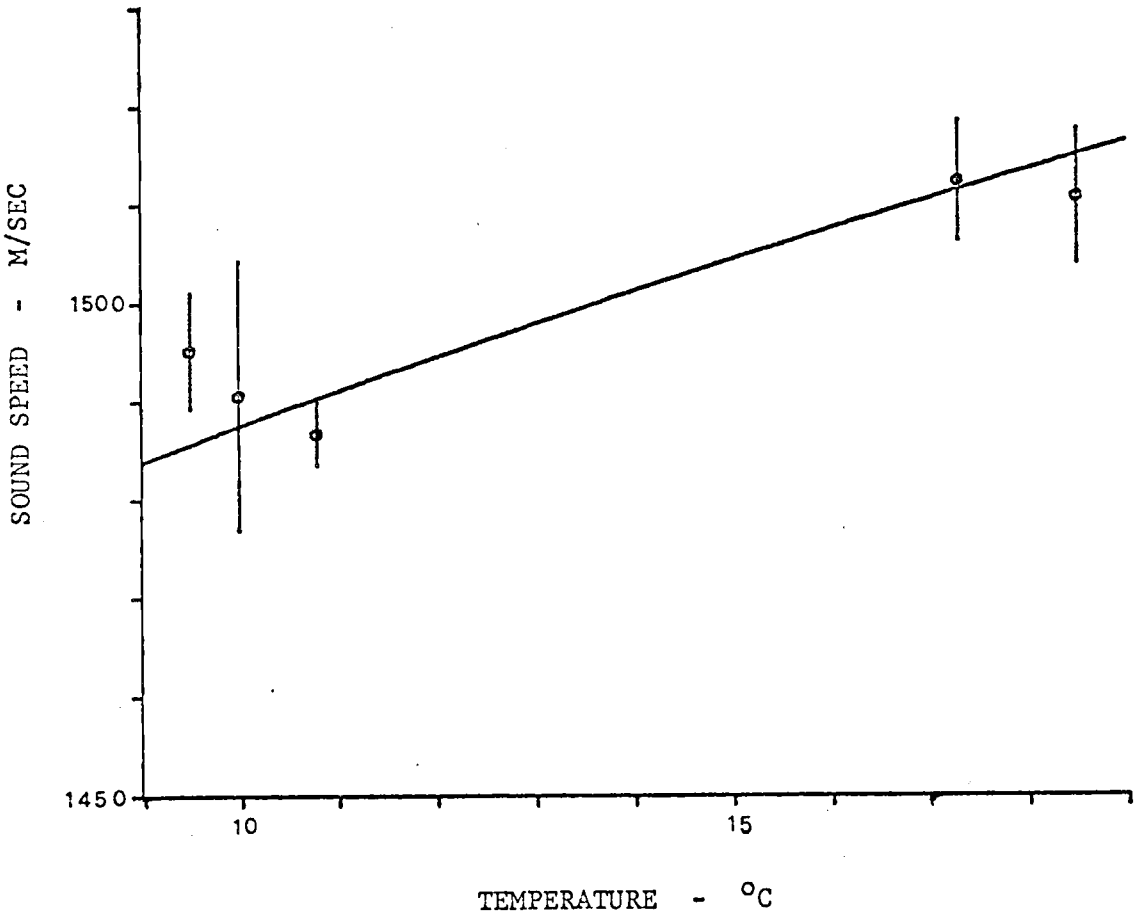

Figure 2. Sound speed versus temperature, copepods.

The solid curve in the figure is sound speed (15) for sea water of 33 $^{o}/_{oo}$ and the temperature of the abcissa, which might be considered typical for the surface waters off Oregon. It is clear that no appreciable sound speed contrast is to be expected if preservation has no effect on the measured sound speeds. For the acoustic measurements in fresh water, there is a significant contrast, of course, which was used in the fluid sphere predictions.

Measurements were made on the euphausiids over a similar temperature range. These results are given in figure 3, again with the sea water sound speed curve for reference. A significant contrast is evident, at least at the higher temperatures. As noted in the description of the apparatus (Appendix), systematic errors are expected at low temperatures so that the low temperature data point should be considered a lower bound estimate of sound speed. The scatter of mean estimates at high temperatures is $\pm$ 7 m/sec, which is about $\pm$ 0.5 percent. Lumping the measurements at laboratory temperature, an estimate of sound speed is 1566.1 $\pm$ 7.8 m/sec at 19.5^{o}C (95 percent confidence interval), the value used in predictions.

Only one series of measurements was made on the sergestids. At 15.8^{o}C, the estimated sound speed is 1545 $\pm$ 5 m/sec, essentially the same as the euphausiids. A good deal of difficulty was encountered in these measurements, as the sergestids were larger than the other specimens and tended to get stuck in the velocimeter bore.

D. Displacement Volumes

Displaced volumes versus length were measured in some detail for

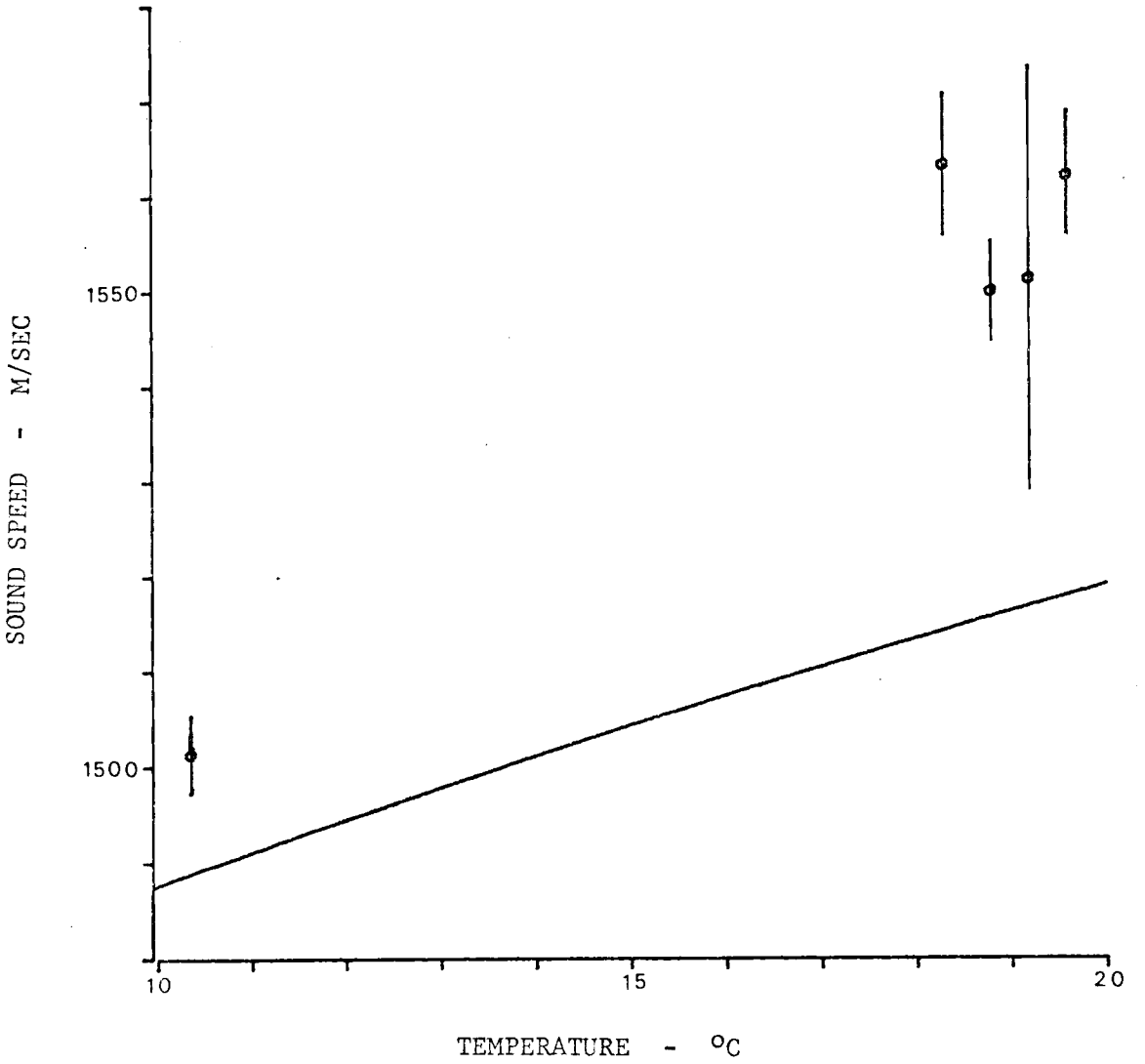

Figure 3. Sound speed versus temperature, euphausiids.

the euphausiids, somewhat cursorily for the sergestids. Copepod volumes were estimated geometrically.

Displacement volumes for the euphausiids were converted to radii of spheres of equal volume, and these radii regressed on (total) length. For 58 specimens[4] between 8 mm and 23 mm in length, the relationship was found.

$$\hat{a} = 0.095 + 0.134\ L\ (mm)$$

where $\hat{a}$ is the radius of a sphere of equal volume and L is the (total) length, both in mm. The coefficient of determination was computed to be $R^2 = 0.975$. (See figure A-1.)

Similar measurements on the sergestids for four specimens between 25 mm and 43 mm gave the regression relation

$$\hat{a} = -\ 0.149 + 0.101\ L\ (mm)$$

with a coefficient of determination, $R^2 = 0.97$.

Displacement volumes for the copepods were estimated geometrically by modelling the body as a prolate spheroid cut in half along the plane containing the axes. The metasome lengths were measured to be 2.5 mm on average, and an eccentricity[5] estimated to be 0.3. The radius of the equivalent volume sphere was estimated as 0.94 mm for these specimens.

---

[4]Eight actual measurements of several specimens each.

[5]Eccentricity, e, is defined by major axis/minor axis ratio: $a/b = e(e^2 - 1)^{-\frac{1}{2}}$.

IV. ACOUSTICAL MEASUREMENTS

A. Acoustical Apparatus

1. Tank

The acoustic measurements were conducted in a glass-walled tank, 1 m x 1 m x 50 cm deep, filled with tap water. A circulation pump and filter system were installed so that the water might be kept reasonably pure. A good deal of trouble was had in eliminating the micro-bubbles in the water. In normal acoustical measurements, these bubbles are of no consequence as their target strengths are quite low. Since the targets to be measured often had lower target strengths than the larger bubbles, however, it was necessary to eliminate them insofar as possible. Eventually, it was found that repeated heating of the tank water to above 40°C and slow cooling to lab temperatures (18 to 20°C) without circulating the water reduced the number of bubbles to negligible levels.

2. Transducers

Ten lead-zirconate-titanate (Channel Industries, 5500 material) ceramic transducer elements were purchased. The resonant frequencies were specified to be 100 kHz to 1000 kHz at intervals of 100 kHz. Each element was a circular piston. The diameters were specified so that all but the lowest frequency element had identical beam patterns (or equal directivity indices of 26.1 dB). From farfield considerations, the lower frequency element was chosen to be smaller, with a

directivity index of 25.1 dB. Half power beamwidths are approximately 10^{o} for all elements.

Each element was cemented into a chloroprene (Armstrong DC-100) boot to provide pressure-release backing. Two housings were fabricated from aluminum, and the elements cemented into recesses machined in the housings. An acoustically transparent window of potting resin (Scotchcast 221) was poured over the active faces of the elements in the housing to waterproof them. Multiconductor cables were provided so that each transducer element could be driven separately. The cases were connected to the cable shield, and the active (outward) faces of the elements were connected in parallel to the ground return for suppression of radio frequency interference.

Each element was used both as a projector and as a receiver to take advantage of the resonance effect of pressure-released ceramic elements. This necessitated the use of a transmit/receive (T/R) switch so that the high transmission drive voltages would not saturate the receiver amplifiers. A satisfactory unit was devised using a line-driver, impedance-transformer integrated circuit with zener diode protected input with an ultra-fast reed relay to short the line-driver output to ground except during a selectable time period. (See Fig. 4 for a block diagram.) An adjustable time delay was provided so that the opening time of the relay might be set to a time when the transmission-induced reactive voltages of the transducer were at sufficiently low levels. After a gain stage, the signals from the transducer (now acting as a receiver) were heterodyned to 100 kHz and passed through a bandpass filter, which remained fixed at the same settings

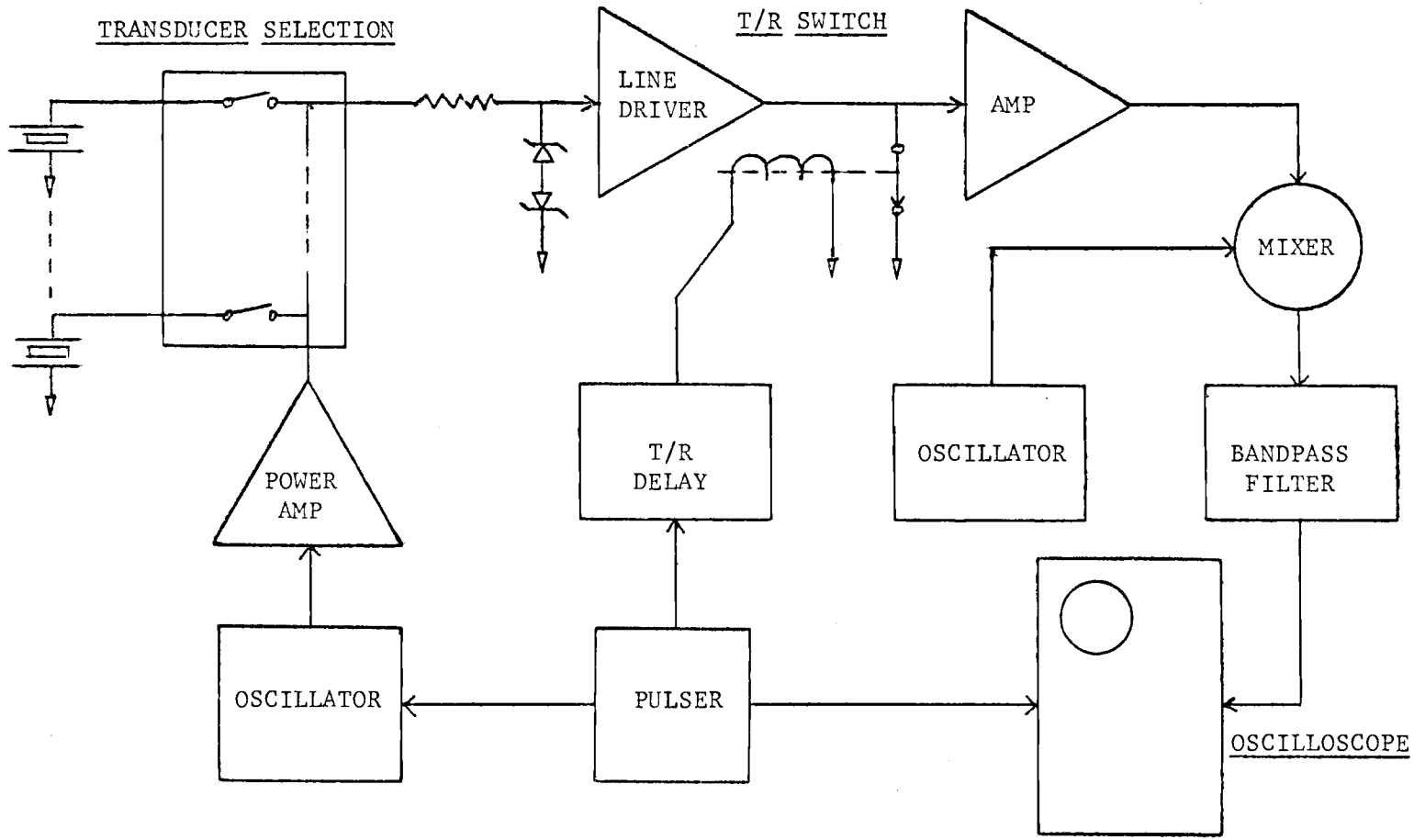

Figure 4. System block diagram.

throughout the measurements. The system gain was measured to be 36 dB ± 1 dB, with a -3 dB bandwidth of 50 kHz, over the frequency ranges actually used. The echo signals were observed on a storage oscilloscope and measured using the graticule marks.

The transmission circuits were conventional; a pulser triggered a gated oscillator to produce nominally 50 μsec sine wave tone bursts that were amplified in a 10-watt power amplifier. A parallel set of reverse-connected diodes was inserted in the high side of the power amplifier output to decouple the relatively low impedance of the power amplifier during reception and to reduce the power amplifier noise contribution.

For convenience in the measurements, the transducer housings were mounted on an aluminum plate that rested on the bottom of the tank via leveling screws at the corners of the plate. This upward-facing configuration reduces the sidelobe interference in a tank wider than it is deep. It also simplified transducer calibration.

Out of ten transducer elements, eight were usable in the measurements. One simply failed to operate (900 kHz). The lowest frequency transducer had an excessively long "tail" on the transmission that extended through the target region and could not be used in this shallow tank. This limited measurements to higher values of ka than were planned. Also, since the frequencies of maximum source level and of maximum receiving sensitivity are different for a given element, the frequencies of optimal operation of the elements differed from the specified resonant frequencies. The eight frequencies available were: 220, 303, 425, 510, 600, 700, 850, and 1100 kHz.

B. Calibration

The transducers were calibrated in a two-step process. A standard hydrophone (Underwater Sound Reference Laboratory model E-8) was used to measure the (voltage) transmitting response over the range of drive voltages available. Especial attention was paid to source levels at low drive levels and the maximum source-level/drive-voltage values. A somewhat larger tank was used for these measurements. Temperatures were comparable to those of the actual measurement tank. Since standard projectors are generally very limited in their useful frequency ranges, and the span of frequencies of the set of transducers was large, a modified version of the self-reciprocity calibration scheme (22) was used to obtain receiving sensitivities.

The transducers were carefully leveled on the plate, and the magnitudes of the surface echo recorded over a range of (low) drive levels. The reflectivity of an air/water interface is essentially unity, so that the target strength, TS, is 0 dB. Writing the sonar equation (23) for this situation

$$TS = 0 = 20 \log(V_S) - (RS + SL) - 20 \log(2r) - 2 \alpha r - G$$

where V_S is the RMS echo level from the surface at range r meters, α is the attenuation coefficient in dB/m, RS is the receiving sensitivity in dB//V/μPa, SL is the source level in dB//μPa at 1 m, and G is the receiving system gain. Since V and r are measurables, and SL is known from the previous calculations, RS may be calculated. The absorption is not negligible at the higher frequencies; however, the form of this equation is essentially that for reducing the actual data

so that $\underline{RS} + 2\underline{\alpha r}$ can be treated as a single quantity, which the surface reflection measurements determine, so long as the test range does not differ too much from the range to the surface.

At drive levels in excess of about 6 or 7 VRMS, the magnitude of the surface echo was too high for linear reception by the elements. Data taken at several values of drive level were plotted so that the nonlinear region could be determined, and linear regression was used on points in the linear region to increase the precision of the estimate of $\underline{RS}$.

Observed echo voltages were reduced to target strengths by the sonar equation applicable to a monostatic sonar:

$$TS = 20 \log(V_z) - (RS + SL) - 40 \log(r_z) - 2\alpha r_z - G$$

where the subscript $\underline{z}$ denotes values for the zooplankter. Depending upon the aspect angle of the specimen being measured, peak or mean values were estimated from the oscilloscope display and recorded for conversion. (See the discussion of the data.) Measurements were usually replicated at least once, the specimen being positioned over each transducer in turn and remeasured.

C. Target Mounting

A variety of specimen mounting schemes were tried. Eventually, it was decided to suspend the specimens over the transducers by a length of very fine leader material (0.08 mm diameter, 0.5 kg test). The upper end of the leader was taped to a bar placed on the sides of the tank, the bar being easily moved to place the specimen over the transducer in use. A single overhand knot secured the plankter to the other

end of the line, and the bitter end was cut at the knot. Examination of the oscilloscope trace for this configuration, without the zooplankter, showed no echo above the noise level at any frequency (although the target strength of the line in normal aspect was not negligible). Occasionally bubbles would adhere to the leader, but this was readily apparent as an extended echo on the scope and the leader could be manipulated to remove the bubbles.

The specimens were kept in a refrigerator (4°C) until they were used, to inhibit bubble formation by the cooling action of the tank water. After each specimen was tied to the leader and placed in the tank, it was examined thoroughly through the glass side of the tank and squeezed and manipulated with tweezers to ensure that no bubbles were trapped in the appendages or under the carapace. The specimens were inspected under a microscope before they were selected to allow those with entrained bubbles (within the body) to be rejected. Bubbles too small to be seen may have been present, but it is thought that the precautions taken make this unlikely.

The copepods were too small to tie onto the leader, so these measurements were made differently. Specimens were transferred from a holding dish of water to the tank with tweezers, held under the surface above the active transducer, and released. Generally, a drop of water encased the specimen during transfer. The monitor scope was placed in storage mode and single sweep. Samples of the echoes were made by manually resetting the sweep trigger at intervals as the copepod slowly sank. Generally, the first samples, obtained while the specimen was near the surface and still near the major response axis of the

transducer, were the best estimates. Data (echo level and time after transmission of the echo arrival) were taken for each sampled echo, whether the copepod was in the beam or had possibly drifted out. Data samples were discarded if the specimen had clearly drifted out of the beam. Many samples were collected at each frequency and converted to TS. The entire range of plausible values is presented in the data plot in the next section.

D. Results

1. Copepods

The measured data for the copepods consisted of estimates that were biased towards low values, as values measured when the specimen had drifted away from the center axis of the acoustic beam would be lower simply because the incident intensity was lower. The best estimates of target strength would tend to be the highest values recorded. Signal to noise ratios were rather low, however, perhaps 6 to 10 dB at the highest frequency, so it is possible that overestimates could be made at the highest frequencies. The entire range of observed values is given in the following data to illustrate the variations encountered, but conclusions are drawn principally on the basis of peak values.

Measured target strengths are plotted against frequency in figure 5. With the exception of the data point at 600 kHz, the trend is for a uniform increase in target strength with frequency over the region of measurements. Geometric estimation of the radius of the equivalent volume sphere gave the value, $\hat{a}$ equal 0.94 mm (Section III. D.). Using

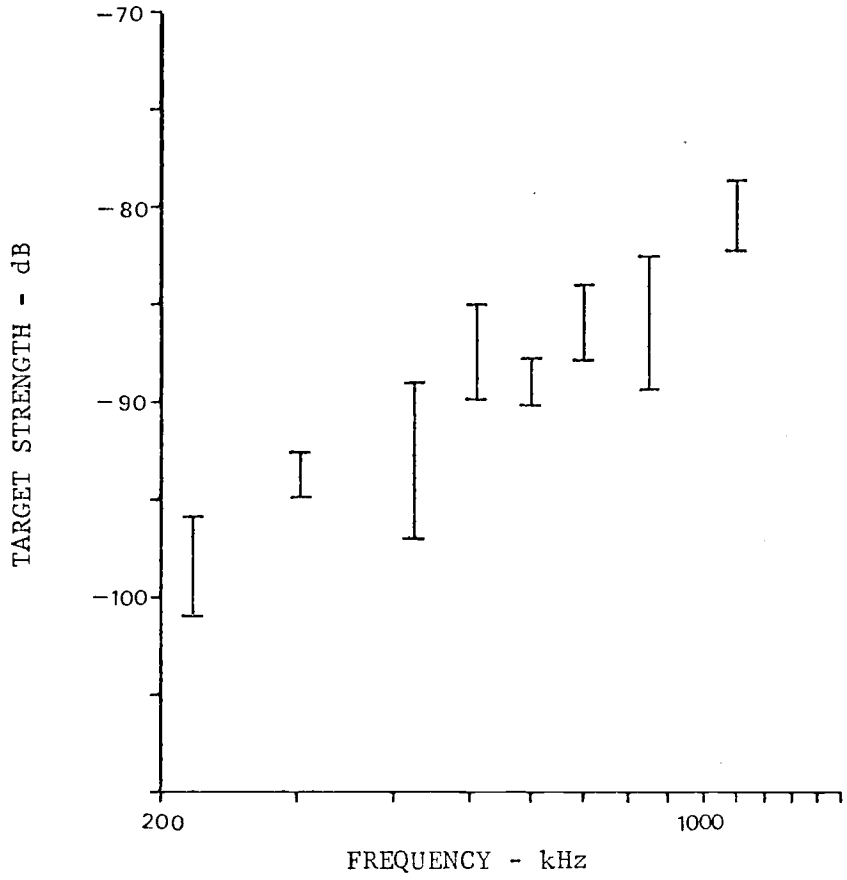

Figure 5. Target strength versus frequency, copepods.

this value, the raw TS data were reduced to TS'. These data are given in figure 6. The solid curve is the fluid sphere prediction of TS' for the measured values of g and h for these copepods (in fresh water). At low ka, below approximately 1.7, the data are lower than the prediction by as much as 6 dB. Above this point, however, the data are consistently higher than predicted. In addition, the trend appears to be a fairly uniform increase, although the predicted null at ka of 2.3 is matched by a (probably fortuitous) small dip at ka of 2.2.

There is no reason to suppose that the appropriate value of $\hat{a}$ to use in reducing the data to the prediction axes must be the radius of the equivalent volume sphere, however. As a first approximation, it is certainly the most obvious, but it is plausible that the nonsphericity of the plankters might be partially adjusted for by altering the value of $\hat{a}$ in some fashion. The corrections applied to the data are not independent, however. If a smaller value of $\hat{a}$ is tried, the data move in both TS' and $k\hat{a}$--up and to the left in this case. A larger value of $\hat{a}$ moves the data down and to the right on the plot. The predicted curve remains fixed, of course.

Replacing $\hat{a}$ with a smaller value, about 0.82 mm, improves the agreement for the lowest four data points, but increases the deviation at high ka (Fig. 7). Any increase in $\hat{a}$ increases the deviation at low ka, where the model might be expected to fit best, with no assurance that the trend towards increase in TS' with ka does not continue so that the curves diverge again. Additionally, it is difficult to conceive how the plankter might scatter like a larger volume than it actually is without postulating resonant behavior.

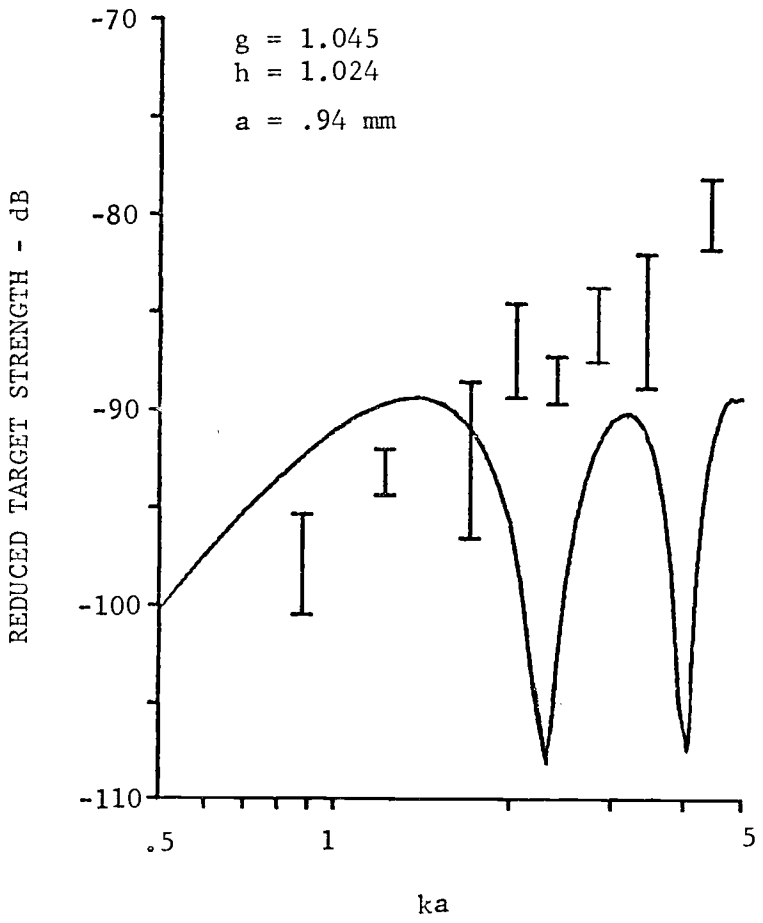

Figure 6. Reduced target strength versus ka, copepods; a = .94 mm.

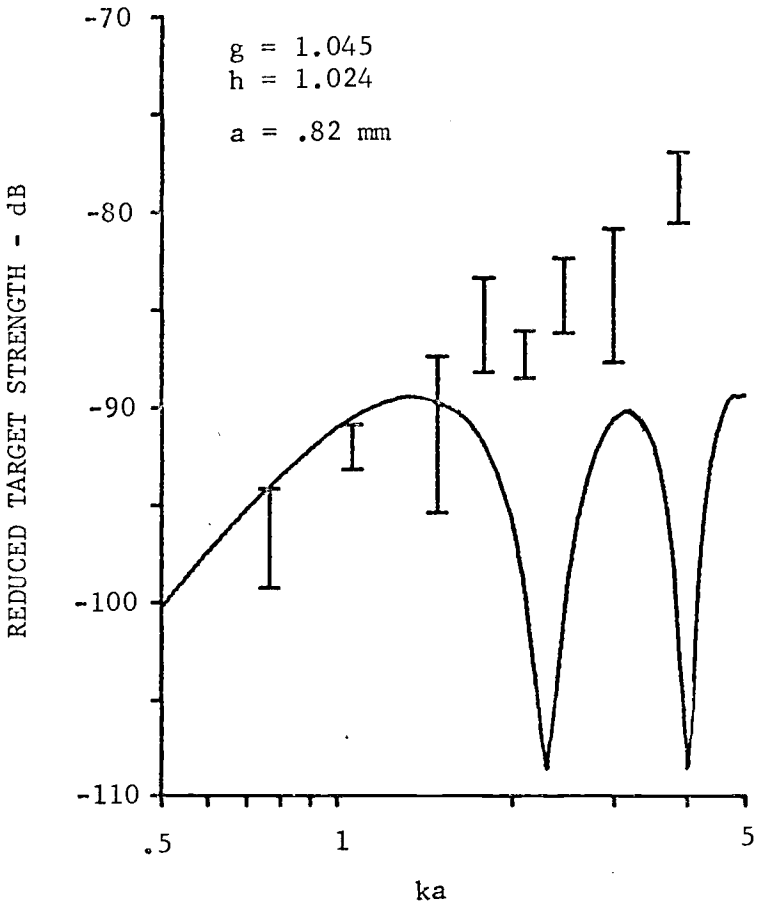

Figure 7. Reduced target strength versus ka, copepods; a = .82 mm.

In the context of the fluid sphere model, it is considered that the reduction in $\hat{a}$ is reasonable and that the deviation from predictions at higher ka is caused by the nonsphericity of the plankter and the resulting lack of higher order spherical modes. That is, for a radius of approximately 85 percent that computed from volume, the fluid sphere model appears to describe the scattering for $k\hat{a}$ in the range of 0.7 to 2 with reasonable precision.

2. Euphausiids

Measurements of target strength were performed on two sizes of euphausiid, 19 mm and 23 mm. A plot of the raw target strength versus frequency data is shown in figure 8. No corrections have been applied to these data. All of the data points shown are for the 23 mm euphausiids. No discernable trends could be found between side and dorsal aspects, so these data are lumped (upper curve). The anterior data were consistently lower, however, so are given separately (lower curve).

It is clear from the differences between dorsal/side aspect data and anterior aspect data that these scatterers are directional. Judging just from the scatter of points, however, it is difficult to determine how directional they might be. The dashed lines drawn in the figure are intended to suggest the best estimates of target strength, based on these assumptions: if the creature is modeled by a finite cylinder, then the best estimate of normal aspect target strength when exact aspect is uncertain is the maximum observed value (given adequate signal to noise ratio). Although the straightest possible specimens were selected, all had some curvature so that dorsal aspects were only

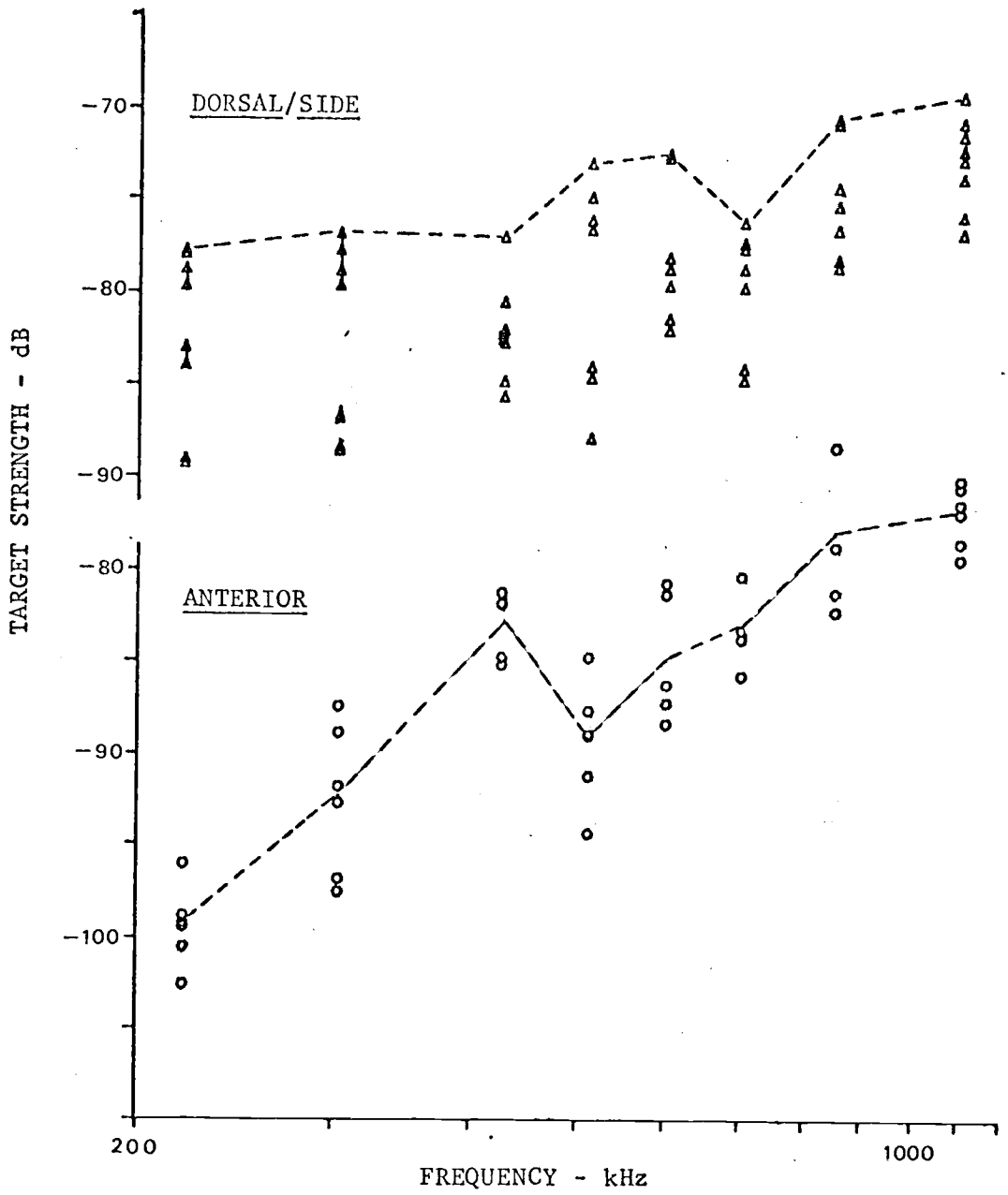

Figure 8. Target strength versus frequency, euphausiids.

approximate. Much imprecision occurred in the suspension also. Thus, the maximum observations of dorsal/side aspect target strengths are taken as the best estimates. Signal to noise ratios generally exceeded 12 dB. Based on areal considerations, it would be reasonable to make a similar argument that the minimum values of target strength observed were the best estimates of the true value of anterior aspect target strength. However, the signal to noise ratios at these echo levels was usually lower than for the dorsal/side aspect data, and it is thought possible that constructive as well as destructive interference could occur due to separate echoes from the head and tail sections. Thus, the best estimates of anterior aspect target strengths are considered to be the mean (geometric, since TS is a log quantity) values.

These targets are clearly directional, the target strength depending upon the orientation of the animal. The fluid sphere, like all spheres, possesses absolute symmetry and cannot exhibit directional backscattering. However, the fluid sphere predicts dorsal/side aspect target strengths pretty well, over a restricted ka range. Figure 9 gives the reduced target strengths, TS', for the dorsal/side aspect data from the 19 mm and 23 mm euphausiids combined. Again, all of the observed values are given even though only the peaks are considered the best estimators. Each point represents a separate positioning over a given transducer, aligned acoustically to yield the highest echo level.

Detailed agreement is not found, of course, and was not expected. The gross behavior is in surprisingly good accord with the predicted

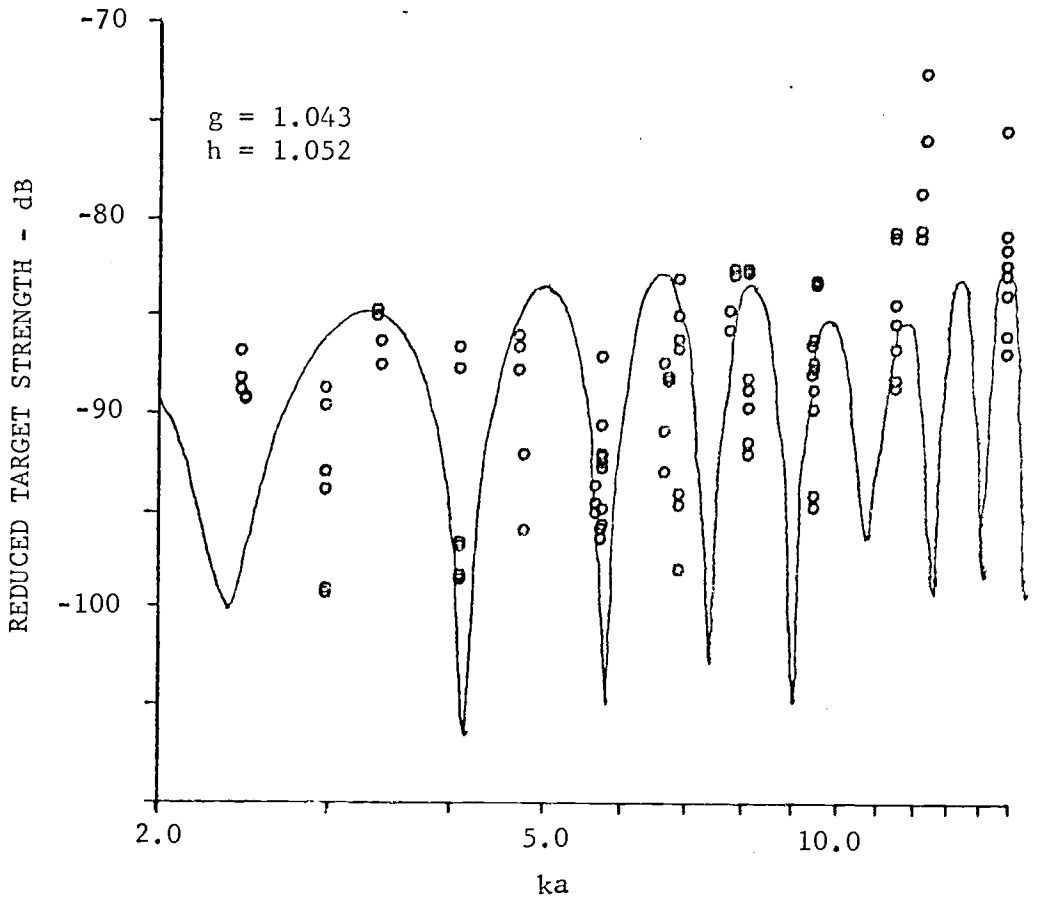

Figure 9. Reduced target strength versus ka, euphausiid.

behavior up to ka approximately 10. The mean levels (of the peaks) are about those of the mean levels predicted; ripples occur, although not as strongly.[6] For any practical purposes, the fluid sphere might be used to predict target strengths (at dorsal/side aspect) over the ka range 2.4 to about 10.

The critical test of agreement would have to include measurements at ka less than 1 however, and these were not possible in this experiment. It must be regarded as possible, then, that agreement is simply fortuitous, and that an entirely different scattering process is occurring. In addition, the fluid sphere cannot predict directivity, and directivity is clearly observed. Finally, the trend is towards higher target strengths at ka approximately 10 (as seen for the copepods at a lower value of ka), implying that the nonsphericity of the scatterer is important at high frequencies.

3. Sergestid Shrimp

Two sizes of sergestid were measured, 31.8 and 34 mm total length. Although larger than the euphausiids, the shapes are rather similar and similar scattering behavior was expected. Only a limited range of $k\hat{a}$ was obtained with the two sizes; using the regression data for $\hat{a}$, the $k\hat{a}$ range is 2.9 to 15.4.

---

[6]It must be noted that the signals possessed finite bandwidth, approximately 20 kHz, and thus the measurements are averages over a range of ka rather than measurements at a point. The ka "bandwidth" for these measurements was 0.25; for the copepods, it was 0.07; and for the sergestids about 0.4. For these comparisons, the finite bandwidth is considered unimportant.

Directivity similar to that seen in the euphausiids was observed for the sergestids, and the subjective opinion was that these specimens were more directional. This would be reasonable for a line-like target where directivity increases with length, although the connection with a fluid sphere becomes more and more tenuous. Target strengths (not reduced) for the 34 mm specimens are presented in figure 10. The upper curve is for dorsal and side aspects, and the lower is for anterior. The general behavior is similar to the euphausiids, but comparisons are difficult with these raw data.

Using the estimate of equivalent volume sphere radius from the regression data, the reduced target strengths, $\underline{TS}'$, were calculated and are shown in figure 11. The limited (and high) range of $\underline{ka}$ makes comparison with the fluid sphere model more difficult. General agreement occurs for $\underline{ka}$ between 2.9 and about 6, and then the trend to higher target strengths begins. Except for the $\underline{k\hat{a}}$ value at which this happens, this behavior is a replica of the deviation from prediction observed for euphausiids and copepods. Again, however, the lack of critical data below $\underline{ka}$ equal 1 allows many alternate scattering hypotheses. The data do show the ability to predict general levels over a small $\underline{ka}$ range, though, and the assumption of continued predictive ability to somewhat lower $\underline{ka}$ is not exceedingly presumptive.

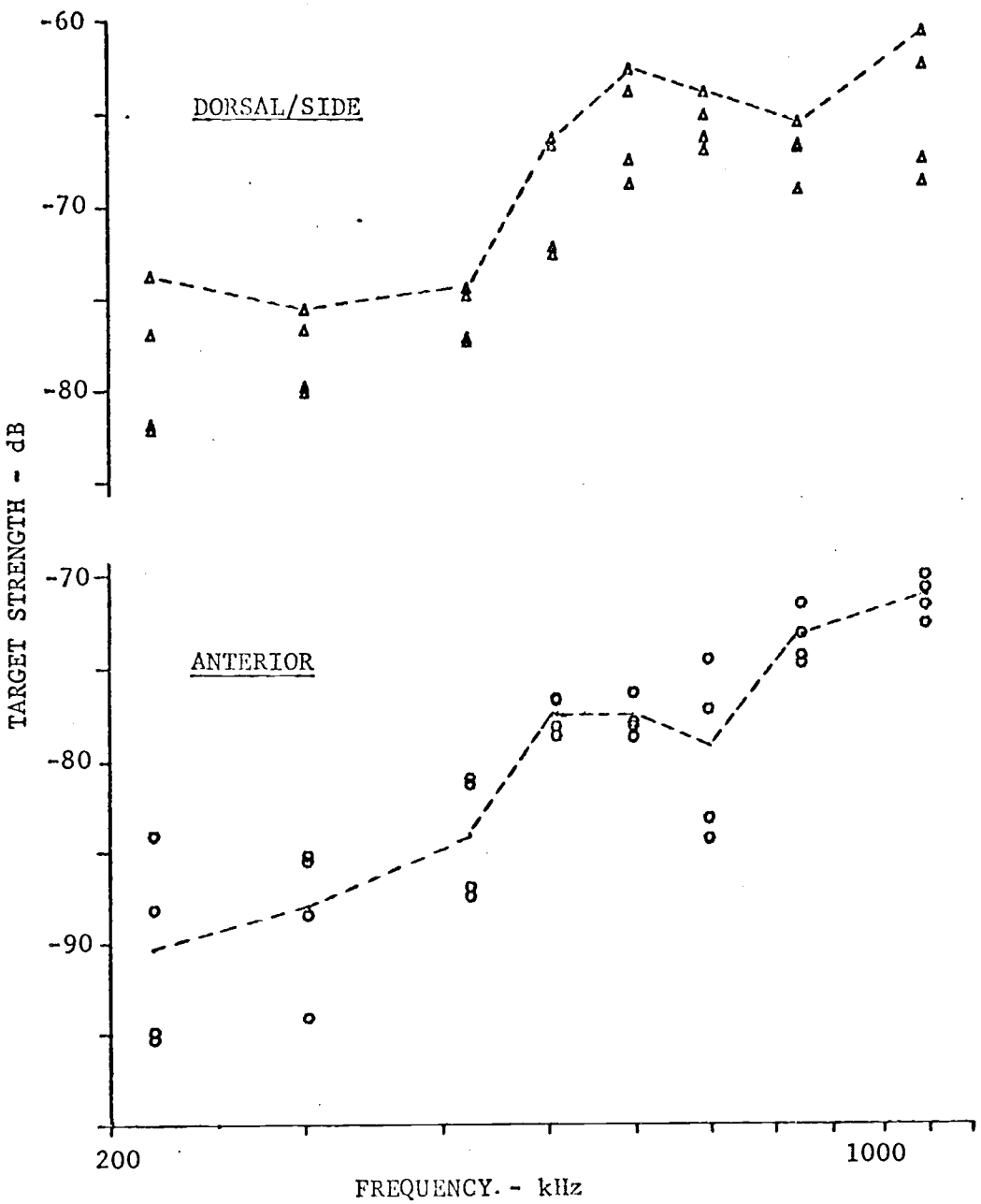

Figure 10. Target strength versus frequency, sergestid.

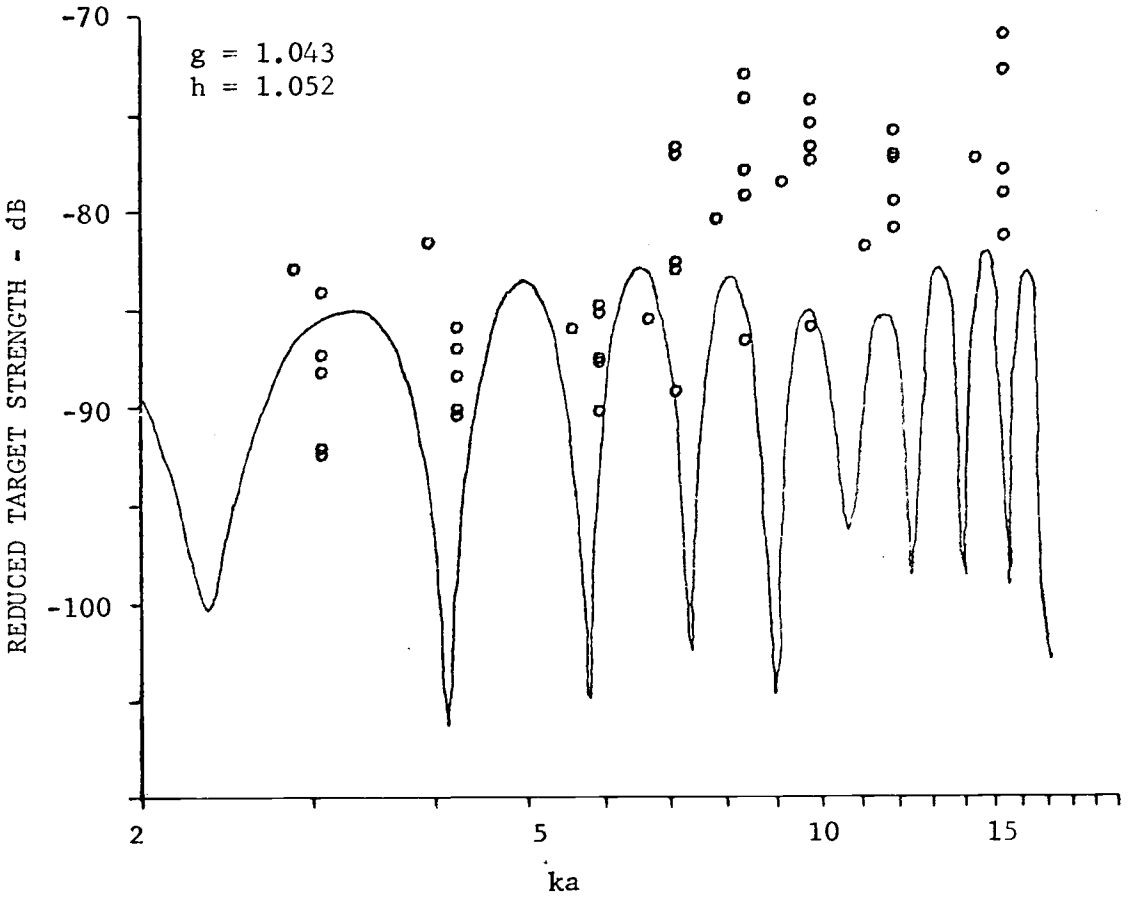

Figure 11. Reduced target strength versus ka, sergestid.

V. DISCUSSION

It is clear from the measurements that although the fluid sphere model provides surprisingly good predictions of target strengths over certain ranges of ka and for normal aspects, much else is occurring that this model cannot describe. For the "most spherical" scatterers, the copepods, the deviation from sphericity becomes important almost as soon as the wavelength and circumference (of the reference sphere) become equal. In fact, for the measurements presented, a straight line of slope 2.4 dB/ka would be adequate--but this would predict higher TS at low ka than either Anderson's or Rayleigh's models and has no geometric scattering analog. The data are well described by such a line, however, and increases over the Anderson model do not occur until ka is less than 0.4.

The agreement of certain ranges of the euphausiid and sergestid target strengths is most surprising in light of their directivity. The directional behavior is also odd--if the targets were acting as line-like targets, the differences between side and anterior aspects ought to increase with frequency as the "line" became more and more wavelengths long. At worst, if the scattering were dependent on the actual cross-sectional areas, the differences would remain essentially constant [TS being approximately 20 log(area/λ)] . The data (figures 8 and 10) show a definite trend for the differences to decrease, contrary to either hypothesis. In addition, the anterior data for the 23 mm euphausiids (Fig. 8, lower) displays a complex behavior with a clear dip at 510 kHz. This suggests interactions of "modes" of vibration

are occurring, but the data are not suggestive of what sort of modes these might be.

The indications are that a single model will not suffice to describe the scattering from all zooplankton without a lot of empirical "rules" and constraints. The data on copepods given here are too meager to shed much light on the appropriate scattering model for these organisms, but the range of $\underline{ka}$ covered is representative of practical echosounding frequencies and typical sizes--so that some predictive use might be made of these data in an empirical fashion.

As a model for the shrimp-like organisms, it is possible that a fluid prolate spheroid would provide useful predictions. This model has not been programmed for comparison (the computational difficulties are not trivial), but there are three reasons which suggest it might be applicable: first, the prolate sphere shape is a better physical representation of the actual shape of these and many other plankters; second, the prolate spheroid will predict directivity, which was observed; third, the fluid prolate spheroid has the fluid sphere as a limiting case of eccentricity (as $\underline{e}$ approaches infinity), so that not very eccentric spheroids would behave much like spheres at low frequencies.

Target strengths *in situ* are expected to be lower than were observed in these measurements since both the density and sound speed contrasts will be reduced in sea water. A correction factor can be estimated by repeated solution of equation 2 for the expected values of $\underline{g}$ and $\underline{h}$ and the values for these measurements (given on figures 6, 9, and 11). The ratio of these $\underline{R}$s estimates the overall level shifts

of the fluid sphere model reflectivities and can be used to estimate the expected changes of the target strengths. Using an *in situ* density of 1.025 gm/ml and the sound speed ratios from figures 2 and 3 (the high temperature ratios were used as best estimates of the ratio; the effect of preservation on sound speed is neglected), correction factors to target strengths were calculated. For the copepods, *in situ* target strengths are expected to be 6.8 dB lower than those measured in fresh water; the euphausiids and sergestid shrimp are about 6.4 dB lower.

BIBLIOGRAPHY

1. Hersey, J. B. and R. H. Backus. 1962. Sound scattering by marine organisms. In The Sea, Vol. I, M. N. Hill, ed. (Interscience, New York): 498-537.

2. Kinzer. J. 1969. On the quantitative distribution of zooplankton in deep scattering layers. Deep-Sea Res., 16: 117-125.

3. Northcote, T. G. 1964. Use of a high-frequency echo sounder to record distribution and migration of Chaoborus larvae. Limn. and Ocean., 9: 87-91.

4. Boden, B. P. and E. M. Kampa. 1964. An aspect of euphausiid ecology revealed by echo-sounding in a fjord. Crustaceana, 9: 155-173.

5. Barraclough, W. E., R. J. LeBrasseur, and O. D. Kennedy. 1969. Shallow scattering layer in the subarctic Pacific Ocean: detection by high-frequency echo sounder. Science, 166: 611-613.

6. Hansen, W. J. and M. J. Dunbar. 1970. Biological causes of scattering layers in the Arctic Ocean. In Proceedings of an International Symposium on Biological Sound Scattering in the Ocean, G. B. Farquhar, ed. (U.S. Gov. Printing Office, Wash., D.C.): 508-526.

7. McNaught, D. C., M. Buzzard, and S. Levine. 1975. Zooplankton production in Lake Ontario as influenced by environmental perturbations. Env. Prot. Agency rpt. EPA-660/3-75-021, June 1975: 40-63.

8. Beamish, P. C. 1971. Quantitative measurements of acoustic scattering from zooplanktonic organisms. Deep-Sea Res., 18: 811-822.

9. Pieper, R. C. 1971. A study of the relationship between zooplankton and high-frequency scattering of underwater sound. Ph.D. dissertation, Univ. of British Columbia: 1-72.

10. Castile, B. D. 1974. Reverberation from plankton at 330 kHz in the Western Pacific. J. Acoust. Soc. Am., 58: 972-976.

11. Smith, P. F. 1954. Further measurements of the sound scattering properties of several marine organisms. Deep-Sea Res., 2: 71-79.

12. Lebedeva, L. P. 1965. Measurement of the dynamic complex shear modulus of animal tissues. Akust. Zh., 11: 197-200. Soviet Physics-Acoustics, 11: 163-165 (1965).

13. Anderson, V. C. 1950. Sound scattering from a fluid sphere. J. Acoust. Soc. Am., 22: 426-431.

14. Strutt, J. W. (Lord Rayleigh). 1878. The Theory of Sound, Vol. II. (Dover Publications, 1945): 272-284A.

15. Medwin, H. 1975. Speed of sound in water: A simple equation for realistic parameters. J. Acoust. Soc. Am., 58: 1318-1319.

16. Machlup, S. 1952. A theoretical model for sound scattering by marine crustaceans. J. Acoust. Soc. Am., 34: 290-293.

17. Yeh, C. 1967. Scattering of acoustic waves by a penetrable prolate spheroid. I. Liquid prolate spheroid. J. Acoust. Soc. Am., 42: 518-521.

18. Hickling, R. 1962. Analysis of echoes from a solid elastic sphere in water. J. Acoust. Soc. Am., 34: 1582-1592.

19. Lebedeva, L. P. 1971. Sound scattering by planktonic animals which are small relative to the wavelength of sound. Oceanology, 11: 890-895.

20. Faran, J. J. 1951. Sound scattering by solid cylinders and spheres. J. Acoust. Soc. Am., 23: 405-418.

21. Ryan, W. W. 1973. Acoustic backscattering from cylinders. Univ. of Texas, Applied Research Lab. rpt. ARL-TR-73-20 (Aug. 1973): 1-78.

22. Patterson, R. B. 1967. Using the ocean surface as a reflector for a self-reciprocity calibration of a transducer. J. Acoust. Soc. Am., 42: 653-655.

23. Urick, R. J. 1967. Principles of Underwater Sound for Engineers. (McGraw-Hill): 16-27.

24. Sweers, H. E. 1971. A comparison of methods used to calculate sigma-t, specific volume anomaly and dynamic height. MTS J., 5: 7-26.

25. DelGrosso, V. A. 1974. New equation for the speed of sound in natural waters. J. Acoust. Soc. Am., 56: 1084-1091.

26. Shmeleva, A. A. 1965. Weight characteristics of the zooplankton of the Adriatic Sea. Bull. Inst. Oceanogr. Monaco, 65: 1-24.

27. Mauchline, J. and L. R. Fisher. 1969. The biology of euphausiids. Adv. Mar. Biol., 7: 284-291.

28. Enright, J. T. 1963. Estimates of the compressibility of some marine crustaceans. Limnol. Oceanogr., 8: 382-387.

29. Greenspan, M. and C. E. Tschiegg. 1959. Tables of the speed of sound in water. J. Acoust. Soc. Am., 31: 75-76.

30. _____. 1966. Handbook of Chemistry and Physics. (47th edition). R. C. Weast, ed. (The Chemical Rubber Co., Cleveland).

APPENDIX

APPENDIX

Acoustical backscattering predictions from the fluid sphere model require knowledge of the densities and sound speeds of the medium and of the scatterer and the radius of the sphere by which the scatterer is modeled. Density and sound speed for the medium may be obtained from tables or published equations (24, 25). Data on zooplankter densities are available in the literature, as are some estimates of volume (26, 27). Enright (28) measured the compressibilities of some marine zooplankters, from which estimates of sound speed can be made. These data are not particularly consistent or even, in some cases (26), believable. Estimates of the density and sound speed for the plankters used in the acoustical measurements were drawn from the literature for preliminary predictions from the fluid sphere model, but actual measurements on the plankters themselves were deemed necessary for useful comparison with the theory.

Conventional techniques were employed to measure displacement volumes and densities. The technique for measuring sound speed is also conventional and is thought to be both simpler and more accurate than the piezometric method employed by Enright. All of these methods ought to be useful at sea on freshly obtained specimens.

Displacement Volumes

As a first approximation, the radius of the sphere which models the zooplankter may be taken as the radius of a sphere whose volume equals the displacement volume of the plankter. The displaced volumes

may be estimated easily by the changes in measured volume of a graduated cylinder partially filled with fluid as specimens of known length are immersed. Single specimens of several tenths of milliliters volume may be measured individually; smaller specimens must be sized first and measured several (of the same length) at a time.

Displacement volumes for very small plankters are probably best estimated geometrically, as the small amounts of water which adhere even to well-drained specimens can be an appreciable fraction of their total volumes. The copepods were measured in this way.

The equivalent-volume-sphere radii measured for euphausiids were regressed on total length (posterior edge of occipital notch to tip of telson) with a first-order linear model. Assumption of this model is equivalent to the assumption that body shape is constant. The equation obtained for measurements of 58 specimens is

$$\hat{a} = 0.095 + 0.134\ L,$$

where $\hat{a}$ is the radius in mm and L is the total length, also in mm. The 95 percent confidence interval estimate for the slope is 0.116 to 0.152. The coefficient of determination is 0.975. A plot of the data is given in figure A-1, together with the regression line. Each point represents the mean value of measurements on a number of individuals. No discernable nonlinearity is evident, implying that the assumption of constant shape is valid.

Density

A simple technique was used for estimating zooplankter densities. Quantities of solutions of different densities were prepared from tap

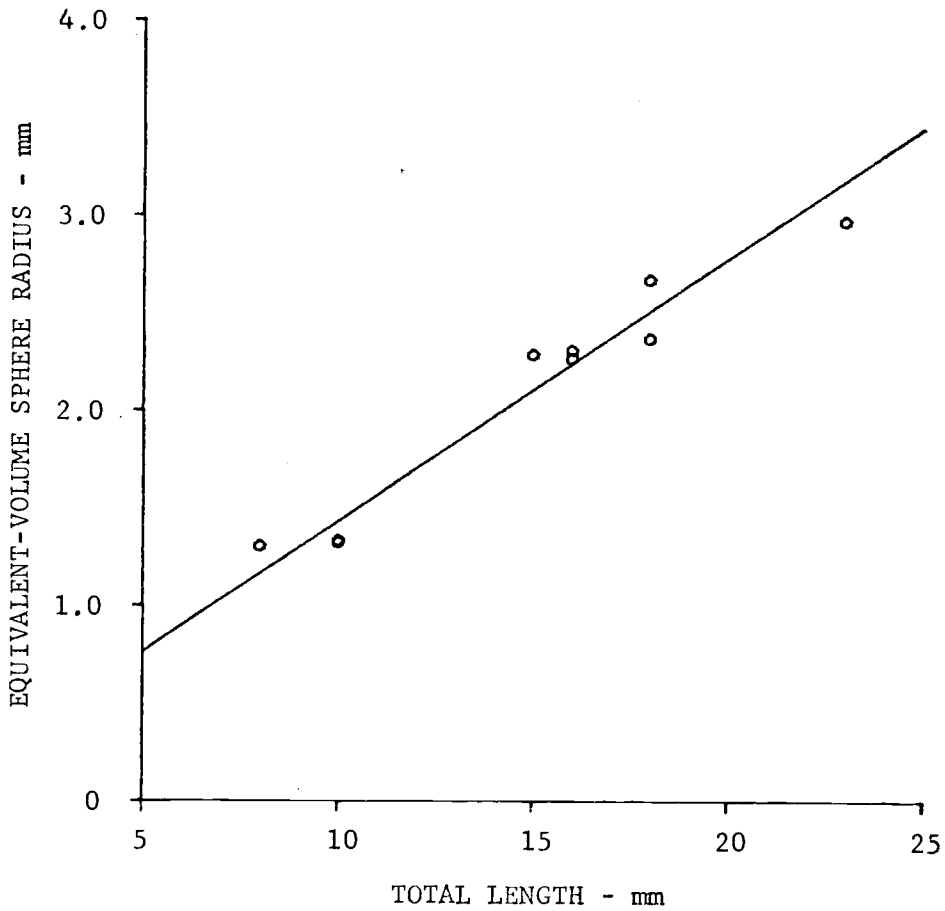

Figure A-1. $\hat{a}$ versus length, E. pacifica.

water and glycerol. Densities of the solutions were measured (as specific gravities, which were taken to be numerically equal) with a laboratory grade hydrometer, with an estimated precision of 0.001. Densities of the solutions prepared ranged from 1.000 gm/ml to 1.075 gm/ml, at intervals of approximately 0.005 gm/ml.

Estimates of density were made in the following way. A specimen was transferred from the preservative to a washing solution of tap water. It was quickly rinsed in this solution to remove the formalin and then placed in a 30 ml beaker of the test solution (one of a series; the first trials were conducted in a solution thought to be more dense than the plankter). If the specimen floated, then its density was less than that of the solution, and it was moved to a beaker containing solution of lower density. Generally, the plankter would sink in one beaker and float in the adjacent one. In this case, the density of the plankter was estimated as the mean of the densities of these two solutions. Occasionally a neutral bouyancy was achieved, and the density of that solution was used as the estimate of plankter density.

Since the density of sea water varies with temperature, it was assumed that a temperature dependence for the plankters existed also. Densities for the euphausiids and copepods were measured at two temperatures, but no significant differences were noted. The measurements were treated as observations from a simple population, and estimates of the mean and variance formed. In all cases, the standard error of the mean was of the order of the interval between density solutions or less--even though apparently real differences existed.

It was concluded that the temperature dependence was less than the precision of the measurement method.

Sound Speed

Sound speed and bulk (adiabatic) compressibility are thermodynamically equivalent measures. Compressibility is a conceptually definable quantity for objects of any size for which classicial thermodynamics applies. Sound speed, on the other hand, is a rather vague concept when applied to objects smaller than a wavelength--such as occurs in the high-frequency measurements presented here. It is, however, the quantity for which the reflectivity equations are written and is somewhat simpler to measure than compressibility.

For a volume of fluid containing objects of slightly different sound speed and density, a good approximation to the sound speed of the mixture is a weighted sum of the sound speed of each. That is, if V_f is the volume fraction of objects with sound speed c', and the fluid has sound speed c_o, then the sound speed of the mixture is approximately given by

$$c = (1 - V_f)c_o + V_f\, c'.$$

This is a linear equation in V_f. Note that the limiting value for V_f approaching 0 is the sound speed of the fluid and the limit as V_f approaches 1 is the sound speed in the objects. This result is the basis upon which the sound speed measurements were made.

A velocimeter was fabricated from two pieces of plexiglas tubing joined in a tee. The horizontal tube contained small, circular-piston transducer elements at each end, jacketed in chloroprene with

a resin window over the active faces for waterproofing. The windows were separated by approximately 50 mm and the volume between used as the sample volume. The vertical tube was of the same diameter (15.9 mm) as the horizontal member and was graduated with a piece of graph paper cemented to the back half-circumference. The transducer elements were identical units (Channel 5500 material) that were on hand; choice of dimensions was largely made around these elements and availability of plexiglas tubing.

Estimation of the sound speed of the fluid in the sample volume was made from the propagation time for a sound pulse to travel from one element (the projector) to the other (the receiver). The projector was driven by a single sine-wave cycle from a gated oscillator. An oscilloscope was triggered by the same pulse used to trigger the oscillator. The sweep was delayed a convenient amount, and the propagation time estimated by the delay time plus the time from sweep start to the pulse arrival. Conversion to sound speed required a knowledge of the length of the sound path. Since an appreciable portion of this consisted of window material of unknown sound speed, it was necessary to calibrate the velocimeter to account for these travel times. The length of the sample volume was measured as carefully as possible, yielding a length of 52.3 mm. The sample volume was filled with distilled water, allowed to equilibrate to lab temperature, and the propagation time measured. The sound speed of distilled water is known as a function of temperature (29), hence the additional delay due to propagation through the resin windows (and delays through the amplifier, fixed delays in the oscilloscope vertical amplifiers, and

errors in the oscilloscope sweep speed) could be calculated.

This calibration was checked by measuring the sound speeds in two other fluids whose sound speeds were known (30). Measurements on ethanol (of unknown purity) yielded a sound speed of 1233.1 m/sec against an expected value of 1187 m/sec; measurements on glycerol yielded a sound speed of 1900.8 m/sec against an expected value of 1893.0 m/sec. The errors were 3.9 percent and 0.4 percent, respectively.

Measurements of the sound speeds for the zooplankters were made in the following way. The sample volume was filled with distilled water up to some even mark on the vertical tube graduations. A baseline value of the propagation time was measured, the temperature measured for determination of the sound speed of the water, and a value for the excess delay time calculated. Drained specimens of the plankter were dropped down the vertical tube into the sample volume, stirred around with a wire to make the distribution approximately uniform, and the propagation time measured. The change in level of the water in the vertical tube was used to estimate the volume fraction of plankters. Only a few specimens were added at a time, so that a series of measurements resulted in data in the form of sound speed versus volume fraction of plankters.

A plot of a typical measurement series is presented in figure A-2. Two features are noteworthy. First, the data do appear to be linear, lending assurance that the assumptions made were valid. Second, the data do not extend to particularly high values of the volume fraction, V_f. The effect of limited volume fractions is to increase the expected

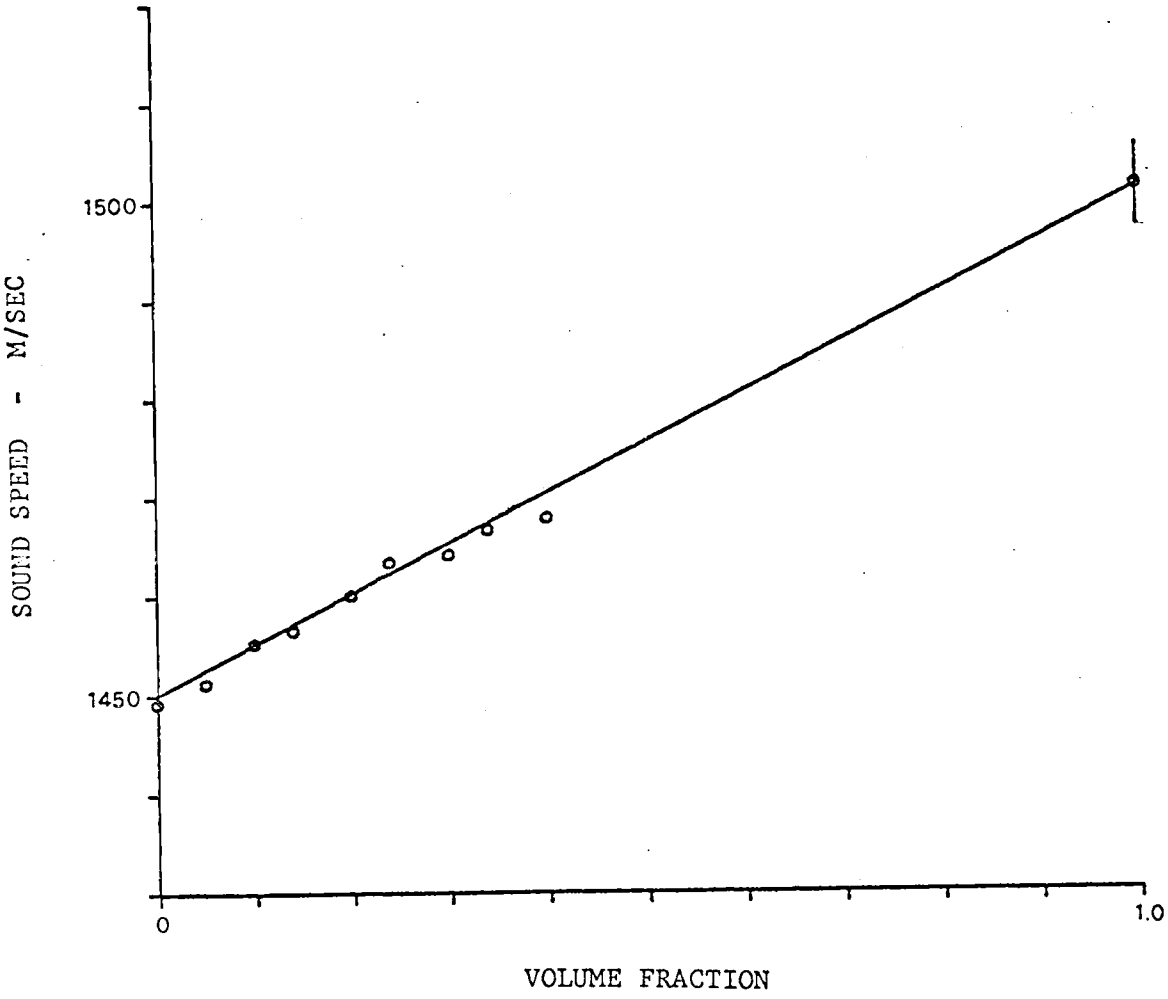

Figure A-2. Sound speed versus volume fraction, E. pacifica at 10.4°C.

error of the estimate of sound speed at a volume fraction of 1, the sound speed of the plankters. A regression line was computed for the data of figure A-2, and this is shown as a solid line on the figure. The sound speed at V_f equal 1 was estimated from the regression equation, as was a 95 percent confidence interval for the expected value (depicted by bars at $V_f = 1$ on the figure).

Sound speed measurements were made at lab temperature for use in the fluid sphere model and at lower temperatures also. The low temperature data is presented in Section III; however, it is thought that systematic errors exist in these measurements, and the data presented are only lower bounds for sound speeds, at best. Calibration with known fluids was not done at the lower temperatures, hence the effect of the contractions of the apparatus are unknown.

Compressibility

Bulk compressibility and sound speed are related by the equation

$$K = 1/(\rho c^2)$$

where ρ is the density of a medium of compressibility K. Enright (28) made measurements of compressibility directly in a piezometer, obtaining an estimate of compressibility of approximately 85 percent that of sea water for preserved specimens of the euphausiid, E. pacifica. Comparison of compressibilities measured by independent methods on specimens of the same species is possible using the data of Section III and the above relation. The density of preserved E. pacifica was measured to be 1.043 gm/ml; sound speed at 19.5°C was 1566 m/sec. Density of sea water may be taken as 1.025 gm/ml and sound speed as

1518 m/sec. Using these values, the compressibility of the preserved euphausiids is calculated to be 92 percent that of sea water at 19.5°C. Presumably this ratio is sensibly constant over limited temperatures, say to the 12°C of Enright's measurements. Enright noted that his apparatus had large and systematic errors, but he did not specify the probable error of his compressibility estimates directly. It is considered that the principal sources of error in the compressibilities calculated from sound speed and density are in the measurements of sound speed, probably less than 2 percent in this case.

The bulk compressibility of preserved euphausiids is estimated to be from 90 percent to 94 percent that of sea water, most probably 92 percent that of sea water. This range of values is substantially in agreement with the independent measurements of Enright.

A similar calculation for the preserved copepods yields a bulk compressibility of 98 percent that of sea water.